

On the Variability of Wind Power Input to the Oceans with a Focus on the Subpolar North Atlantic

XIAOMING ZHAI

School of Environmental Sciences, University of East Anglia, Norwich, United Kingdom

CARL WUNSCH

Department of Earth, Atmospheric, and Planetary Sciences, Massachusetts Institute of Technology, Cambridge, Massachusetts

(Manuscript received 23 July 2012, in final form 1 December 2012)

ABSTRACT

Variations in power input to the ocean using a recent global “reanalysis” extending back to 1871 show a strong trend in the net power input since then, a trend dominated by the Southern Ocean region. This trend is interpreted as a spurious result of the changing observational system. Focusing therefore on the North Atlantic Ocean, where the database is somewhat more secure, it is found that the input power in the subpolar North Atlantic varies significantly in time, showing a strong relationship to the North Atlantic Oscillation (NAO). During positive NAO index years, power input is greater owing to enhanced synoptic activity. Furthermore, cumulative power input to the subpolar North Atlantic is found to correlate significantly with both the eddy kinetic energy there and the Atlantic multidecadal oscillation (AMO), although the physical mechanism at work remains unclear. The assumption that the changing ocean can be neglected relative to the changing atmosphere in calculating the power input is found to be a usefully accurate approximation over the two decades for which changing ocean state estimates are available. Strong dependence on synoptic weather systems of monthly-mean stress distributions implies that past and future climate simulations must account properly for changes in weather systems, not just the large-scale variations.

1. Introduction

An understanding of the forces powering the ocean’s circulation is a useful diagnostic of the governing physics and a strong indicator of how the system might respond to shifts in their structures and magnitudes. The present understanding is that wind systems are the dominant energy source, followed by tides (for the abyssal circulation) and buoyancy exchanges with the atmosphere. Quantitative determination of power inputs from winds and buoyancy exchange is complex in part because it depends upon knowing a great deal about the circulation set up by those same forces.

Thus energy is input to the ocean where wind and ocean surface flows are aligned, and energy is removed where they counterflow, with the flow being determined

mainly by the wind field itself. The input of buoyancy-derived power has been generally regarded as comparatively weak (e.g., Wunsch and Ferrari 2004). It is now clear that the degree of energy input from buoyancy driving depends sensitively upon the independent existence of a wind-forced circulation. Mechanical driving catalyzes the injection of buoyancy power. This result is clearest in both one- [e.g., Wunsch 2005, his Eq. (34)] and two-dimensional [e.g., Hazewinkel et al. 2012, their Eq. (1.9)] systems and is presumed to be similar in three dimensions. Total wind power input is generally always positive, while that from buoyancy forcing can be of either sign, as various authors have estimated.

In addition to arguments deriving from calculated power input, simple analytical theories show that shifts in the wind field lead to a complex oceanic reactions on time scales ranging from hours (top-to-bottom barotropic motions) to baroclinic adjustments over years, decades, and longer. Despite the very long time scales required for complete oceanic adjustment, a host of observations, as well as theory, shows that major parts of

Corresponding author address: Xiaoming Zhai, School of Environmental Sciences, University of East Anglia, Norwich NR4 7TJ, United Kingdom.
E-mail: xiaoming.zhai@uea.ac.uk

the ocean are capable of extremely rapid responses to changing wind patterns. For this reason, attempts to understand the changing ocean circulation on all instrumentally accessible time scales logically start with an understanding of how the wind has changed and how the ocean reacted.

The purpose of this present study is to explore the degree to which the net input of power to the ocean's circulation varies through time, and whether that time variation gives rise to observable and important changes in the circulation. Discussion is confined to the wind component, both because it appears dominant and because, in contrast with the buoyancy forcing, its determination does not depend upon knowledge of the interior circulation.

For reasons outlined below, primarily involving the extreme lack of useful observations of both atmosphere and ocean, this analysis must be regarded as directed at determining orders of magnitude but, as will be seen, pointing to the importance of the concepts. A few studies exist of the time-varying energy input into the ocean's circulation. An example is Huang et al. (2006), who inferred a global wind power input varying greatly on interannual and decadal time scales using National Centers for Environmental Prediction (NCEP) and European Centre for Medium-Range Weather Forecasts (ECMWF) reanalysis products, with an apparent increase of about 12% over the past 25 years. Recently, Brown and Fedorov (2010) examined power input to the tropical Pacific Ocean on ENSO time scales and found a strong interannual variability in apparent power input, with less power input during El Niño years.

The ocean's circulation is global, with presumed but poorly understood, and almost unquantified, transmission of energy input in some areas to large distances. That the local wind work on parts of the global circulation is negative on the average (see Fig. 3 of Zhai et al. 2012) immediately implies that the energy to sustain the known motions in those places must be provided from elsewhere or by other mechanisms. Serious issues arise concerning wind field estimates over much of the World Ocean, largely deriving from the near absence until recently of direct observations.

2. Methods

The rate of work P (power) by the atmosphere on the ocean (and vice versa) is computed from the inner product,

$$P = \boldsymbol{\tau} \cdot \mathbf{u}, \quad (1)$$

where \mathbf{u} is the surface velocity and $\boldsymbol{\tau}$ is the vector stress exerted by or on the atmosphere. From arguments

apparently first outlined by Faller (1966) and Stern (1975), the power input to the geostrophic circulation can be computed accurately by replacing \mathbf{u} by its geostrophic component \mathbf{u}_g . Because wind fields are so variable (as is \mathbf{u}_g to an extent), Eq. (1) is only meaningful when computed over some interval long relative to the synoptic wind scales, and is thus replaced by

$$P = \langle \boldsymbol{\tau} \cdot \mathbf{u}_g \rangle, \quad (2)$$

where the averaging time in the angle brackets is left indefinite for the moment.

Zhai et al. (2012) discuss the difficulties in computing $\boldsymbol{\tau}$ —the usual quadratic drag laws produce a very strong dependence upon the synoptic wind variability and accurate estimates cannot be computed from the weekly- or monthly-mean wind fields. The now much-discussed systematic effects of the moving ocean also have an important quantitative impact on conventional drag-law formulations (Duhaut and Straub 2006). Readers are referred to Zhai et al. (2012) for a physical illustration of this moving ocean effect in the stress calculation. However, because of lack of data, this moving ocean effect is not taken into account in the present study; the accuracy of estimates of the variability of power input without the moving ocean effect is tested for the period 1995–2008 at the end of section 3. Because the drag laws are turbulent parameterizations, the shortest time interval over which they can be employed with atmospheric winds is also unknown. Roquet et al. (2011) show furthermore that, in a balanced state, the regions where P is actually injected into the geostrophic circulation can differ significantly from those places where P is generated, owing to the lateral energy transfer in the Ekman layer.

Note that what we call the “resting ocean approximation” refers only to the neglect of the oceanic surface flow in the calculation of $\boldsymbol{\tau}$. No work can be done by the wind on the ocean unless the latter is in motion.

a. Reanalyses

Global estimates of the rate of wind work on the ocean, and its temporal variability, depend upon accurate stress estimates. The meteorological community has, for some years, been producing global-scale estimates of the atmospheric state that are called “reanalyses.” Originally restricted to intervals on the order of 50 years into the past, they have now been extended back to 1871 (Compo et al. 2011). Although interesting and to some degree useful, a large number of studies (e.g., Trenberth et al. 1995, 2001; Bengtsson et al. 2004; Bromwich and Fogt 2004; Bromwich et al. 2007, 2011; Nicolas and Bromwich 2011) have shown serious discrepancies among these products, even in the

recent past. In particular, a number of these published papers have cautioned in strong terms against using the reanalyses for any sort of trend determination. Wunsch and Heimbach (2013) have summarized the list of issues, both physical and numerical, that undermine the utility of these products for climate studies.

If a single major issue is to be identified, it is the extreme changes in the nature and distribution in space and time of the atmospheric observing system. Where data are comparatively sparse today, qualitative differences exist between reanalysis products, all using the same data. If reliable estimates can be made as long ago as 1871 from the sparse measurements available at that time, climate measuring systems for determining future change can be much thinner and cheaper than those required for weather forecasting.

Owing to its extended duration, this present study begins with the Compo et al. (2011) reanalysis. The particular reanalysis product was produced by assimilating surface pressure observations from the International Surface Pressure Databank and using sea surface temperature (SST) and sea ice concentration fields from the Hadley Centre Sea Ice and SST (HadISST; Rayner et al. 2003) dataset as model boundary conditions. It has a temporal resolution of 6 h and spatial resolution of 2° .

For analysis purposes, two types of stresses are used in Eq. (2). The first type is the monthly-mean wind stress τ taken directly from the Compo et al. (2011) reanalysis. Note that the monthly-mean stress is a monthly average of the instantaneous stress, therefore including contributions from both synoptic winds and monthly winds in the quadratic stress law. The second type is the stress computed from the reanalysis using a stress law (Large et al. 1994) and winds averaged over a month τ_m (i.e., stress owing to monthly winds alone). Power input from τ and τ_m are then computed using Eq. (2) and are labeled P and P_m , respectively.

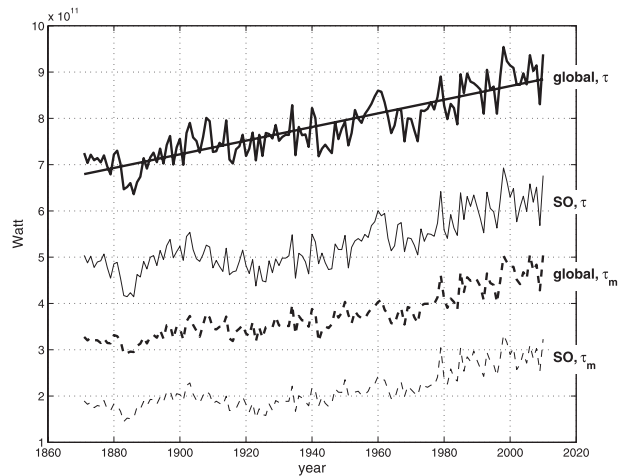


FIG. 1. Power input to the global ocean (thick lines) and the Southern Ocean (SO; thin lines) for the period 1871–2010, estimated using the monthly wind stress τ (solid lines) and stress owing to monthly winds τ_m (dashed lines) from 20CR (Compo et al. 2011). The straight line shows the linear trend of the global wind power input for this time period.

b. Surface flow

More or less reliable oceanic surface geostrophic flow estimates do not become available until the advent of high-accuracy altimetry beginning in 1992. The Estimating the Circulation and Climate of the Oceans (ECCO) estimates (Wunsch and Heimbach 2013) combining the altimetry with hydrography and many other data types also adjust the reanalysis surface wind stress and other meteorological fields to make them consistent within error bars of the oceanic data in a system free of artificial forces and sources and sinks. Although similar analyses preceding 1992 exist (Wang et al. 2010), they suffer from the same paucity of data as do the atmospheric reanalyses and are thus little more than examples of physically possible oceanic states rather than being reliable estimates of the actual state. (Some skill in the years

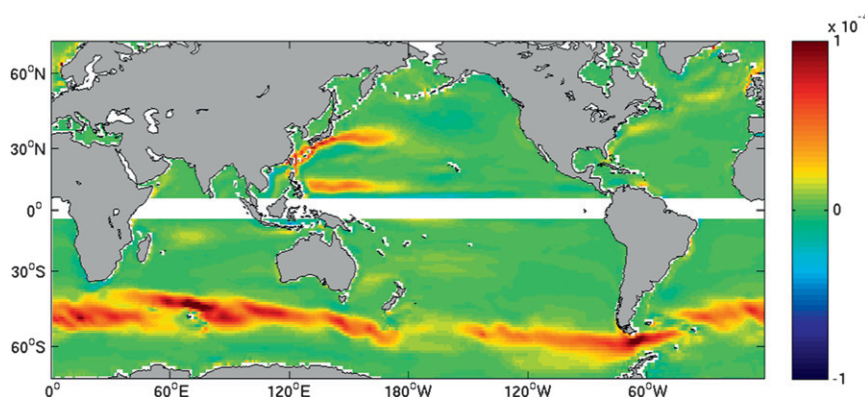


FIG. 2. The linear trend of global power input for the period 1871–2011 ($\text{W m}^{-2} \text{yr}^{-1}$).

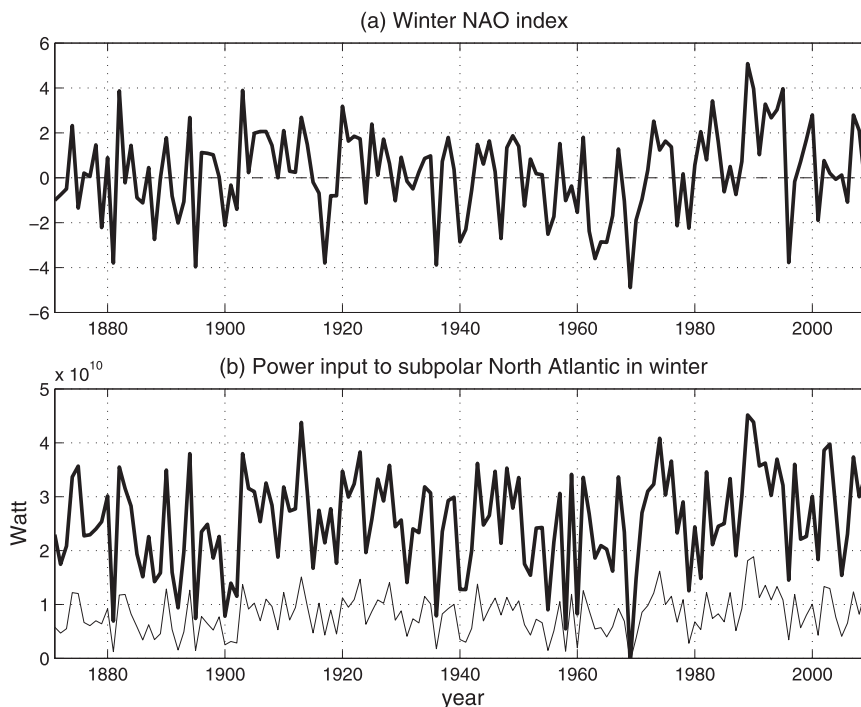


FIG. 3. (a) The winter NAO index provided by the Climate Analysis Section of NCAR (Hurrell 1995). The winter NAO index is based on the difference of normalized sea level pressures between stations in Lisbon, Portugal, and Stykkisholmur/Reykjavik, Iceland, averaged from December to March. (b) The thick line is the power input to the subpolar North Atlantic P estimated using monthly stress from 20CR, whereas the thin line is the power input owing to stresses calculated from monthly winds P_m .

preceding altimetry is expected from the “backwards in time” propagation of information, but the upper ocean is so volatile that the detailed surface flow is mainly dependent upon the accuracy of the near-instantaneous wind field.)

In the spirit of what can only be an order-of-magnitude estimate of power input through time, the analysis will be done initially by assuming that the ocean circulation has remained constant since 1871, using the time average of ECCO sea surface height from 1992 to 2008.¹ An estimate will then be made, using the ECCO fields, and the raw altimetry, of the influence of the time-varying ocean circulation: it is found to be of secondary importance only.

c. Power input 1992–2011

For the period from October 1992 to December 2011 when the high-accuracy altimetry data are available, the

total sea surface height (SSH) can be obtained by combining the time-mean SSH from ECCO and the SSH anomaly product compiled by the Collecte Localisation Satellites (CLS) Space Oceanography Division of Toulouse, France. The SSH anomaly values result from merging the Ocean Topography Experiment (TOPEX)/Poseidon and *European Remote Sensing Satellites 1 and 2 (ERS 1/2)* along-track SSH measurements for a temporal gridding of 7 days on a $1/3^\circ$ Mercator grid (Le Traon et al. 1998). Note that altimeter SSH anomalies are used here, rather than SSH anomalies from ECCO, to obtain higher resolution. The mean SSH from ECCO is interpolated from a 1° latitude–longitude grid to the same grid as the SSH anomalies. Surface currents \mathbf{u}_g are then computed through geostrophy from the total SSH with temporal resolution of 7 days. For the period 1992–2011, the NCEP reanalysis wind product (Kalnay et al. 1996) is used to compute power input from τ and τ_m after being interpolated to the same grid as \mathbf{u}_g .

Zhai et al. (2012) showed that time variability in the ocean surface velocity is unimportant in computing the time-averaged wind power input. As will be seen later,

¹ We here use the mean surface flow as determined from ECCO, version 3.73, for computation of the power input. A comparison with the use of the Maximenko and Niiler (2005) mean sea surface showed differences that are much smaller than the uncertainty of the wind product (not shown).

changing ocean circulation [i.e., \mathbf{u}_g in Eq. (2)] is also only of secondary importance to calculations of the variations in wind power input: they are dominated by the changing wind stress, not the changing ocean circulation, at least on the accessible time scales.

In summary, the moving ocean effect in the stress calculation is not considered in the present study. For the period of 1871–2010, power input is calculated using the Twentieth Century Reanalysis (20CR) wind product and time-invariant ocean circulation obtained from the averaged ECCO state. For the period of 1992–2011, power input is calculated using the NCEP reanalysis wind product and time-varying ocean circulation obtained from combining the averaged ECCO state and altimetry data. In addition, the accuracy of estimates of the variability of power input calculated by ignoring changes in the oceanic surface flow is tested for the period 1992–2011 by comparing power input estimated with the steady ocean circulation approximation with that estimated without. The accuracy of estimating the variability of power input without the moving ocean effect in the stress calculation is also tested for the period 1995–2008 by comparing power input estimated with the moving ocean effect with that estimated without.

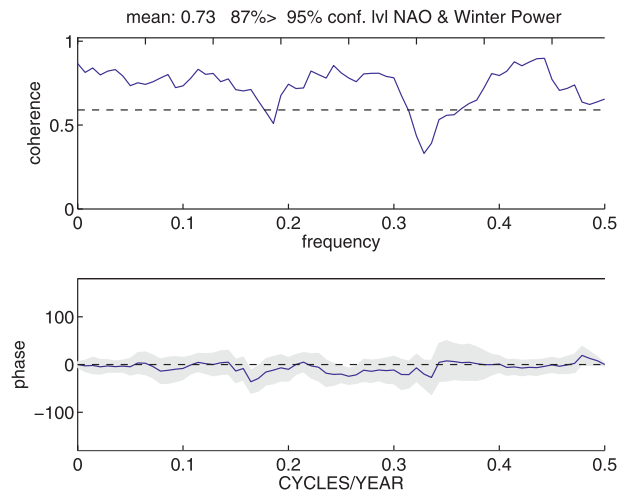


FIG. 4. (a) Coherence and (b) phase between the winter NAO index and power input to the subpolar North Atlantic. The dashed line in (a) is the 95% confidence level.

3. Results

a. Global results 1871–2010

Consider first the global results. If taken literally, Fig. 1 shows that the global power input (the thick solid

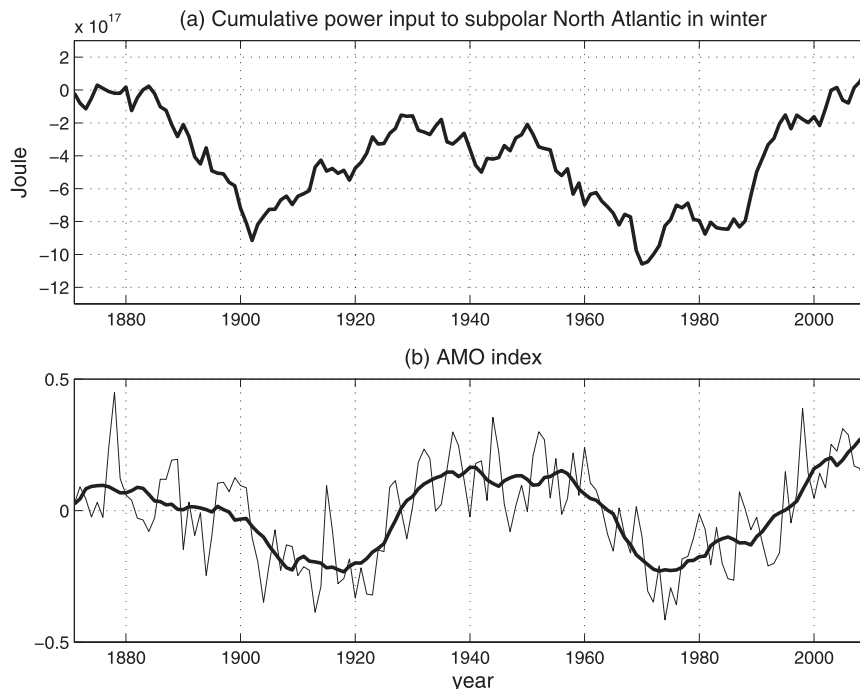


FIG. 5. (a) The cumulative power input Π to the subpolar North Atlantic in winter. Note that the time-mean value is removed before cumulation. (b) The AMO index is taken from the Physical Sciences Division of the National Oceanic and Atmospheric Administration (Enfield et al. 2001). The thick line is a 10-yr running average.

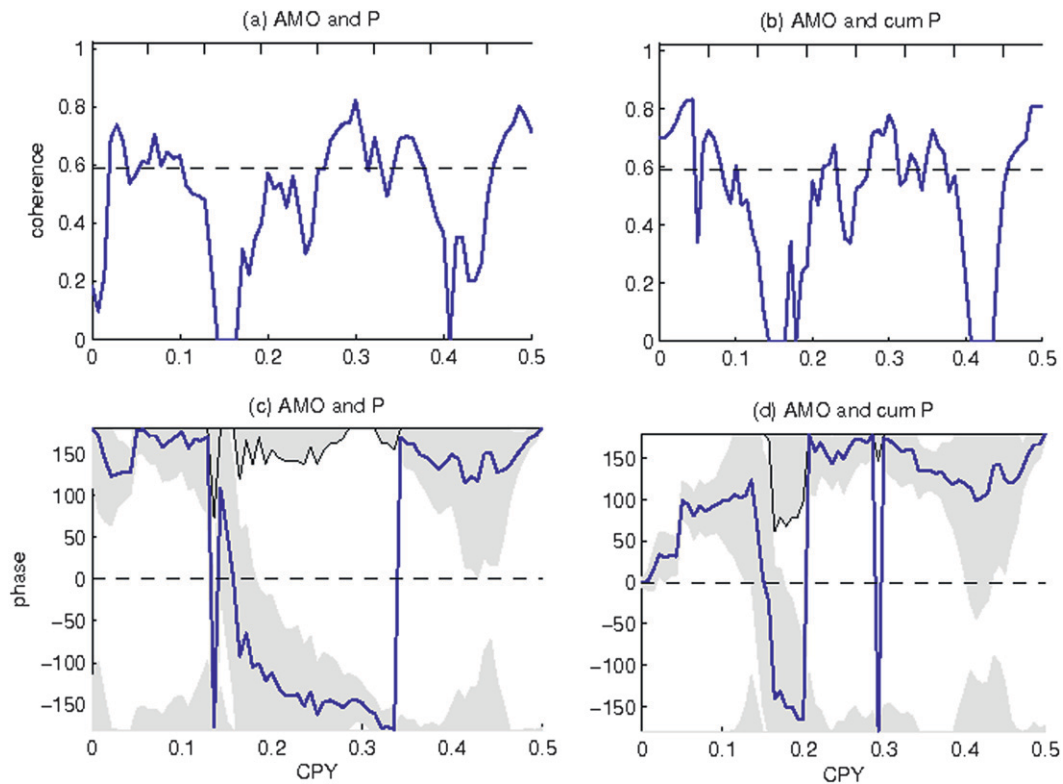


FIG. 6. (a) Coherence and (c) phase between power input to the subpolar North Atlantic and the AMO index. (b),(d) As in (a),(c), but for coherence and phase between Π and the AMO index. The dashed lines in (a) and (b) are the 95% confidence level. Positive phase in (c) and (d) means the AMO index lags.

line) has increased by over 30% over the last 140 years, with a linear trend of $\sim 1.5 \times 10^9 \text{ W yr}^{-1}$. The time-mean global P over the last 20 years is $\sim 8.9 \times 10^{11} \text{ W}$, roughly consistent with previous estimates (e.g., Wunsch 1998; Hughes and Wilson 2008; Scott and Xu 2009; Zhai et al. 2012), while the time-mean global P over the whole 140 years is only $\sim 7.8 \times 10^{11} \text{ W}$. If this increase in global P from 1871 onward is real and not an artifact of the changes in observations, it would have profound implications for ocean circulation changes over the last 140 years including, for instance, a significant increase in gradients of the dynamic topography.

The global power input owing to wind stresses calculated from monthly winds P_m is also plotted in Fig. 1 (the thick dashed line). Although the mean values are much lower, the trend in global P over the period 1871–2010 is also seen when using stresses calculated from monthly winds; synoptic winds apparently play only a secondary role in the calculated increase with time. Figure 2 shows the map of the linear trend of global P over the last 140 years, where the most significant increase is found in the Southern Ocean and Kuroshio region. Power input in the Southern Ocean between 65° and 30°S (the thin solid line in Fig. 1) indeed dominates the trend and variability

of global P . After separating contributions from synoptic and monthly winds in the Southern Ocean, the trend in stresses owing to monthly winds τ_m in the Southern Ocean is found to explain most ($\sim 60\%$) of the trend in global P over the last 140 years.

This trend is almost surely an artifact, as the Southern Ocean is probably the most poorly observed region of the World Ocean, even today. Notice that the increase in wind power input seems to coincide with the end of World War II and probably is the result of a greatly increased observing system built up shortly after that. Apparent wind trends in the various modern reanalyses also differ qualitatively over the Southern Ocean (D. Bromwich and J. P. Nicolas, Ohio State University, 2010, personal communication). Pending the appearance of independent confirming evidence, prudence dictates regarding the gross change in power as spurious.

b. Subpolar North Atlantic 1871–2010

Consider now, instead, the North Atlantic Ocean, a much smaller region with an imperfect but considerably better data coverage than has been available for the Southern Hemisphere. In the North Atlantic, the

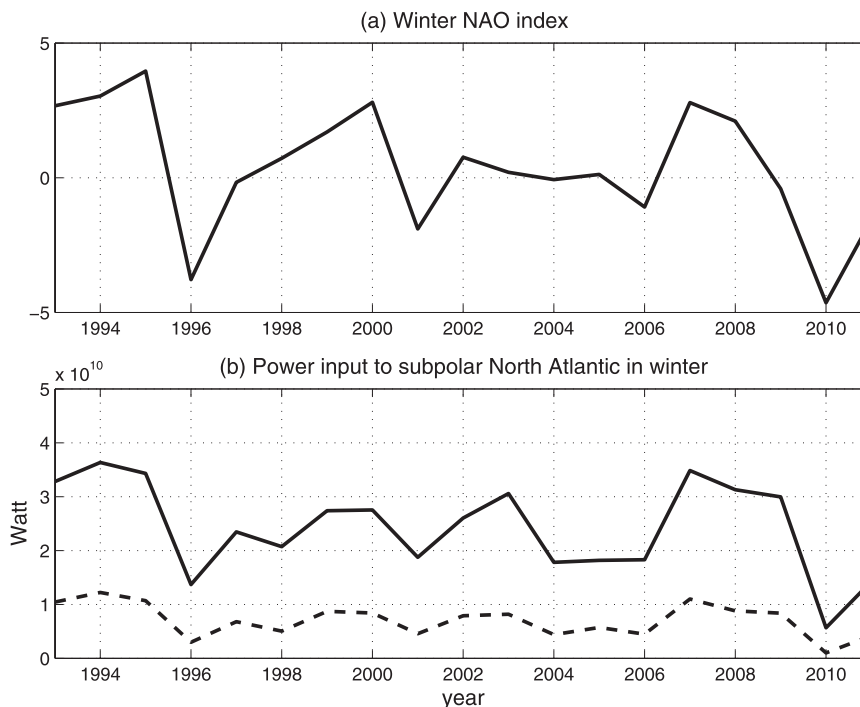


FIG. 7. (a) The winter NAO index. (b) The solid line is power input P to the subpolar gyre in the North Atlantic in winter, while the dashed line is power input to the subpolar gyre in winter owing to monthly winds P_m .

strength and location of the westerly winds and storm activities are known to exhibit large year-to-year variability, depending on the phase of the North Atlantic Oscillation (NAO; Hurrell 1995). Positive values of the NAO index are typically associated with stronger-than-average westerlies over the midlatitudes and more intense weather systems over the North Atlantic. Figure 3a shows the winter NAO index provided by the Climate Analysis Section of the National Center for Atmospheric Research (NCAR) (Hurrell 1995). The winter NAO index is based on the difference of normalized sea level pressures between stations in Lisbon, Portugal, and Stykkisholmur/Reykjavik, Iceland, averaged from December to March. Note that the stations are fixed in space and thus may not track the movement of the NAO centers of action.

The thick line in Fig. 3b shows the annual winter-mean power input P to the subpolar gyre in the North Atlantic. The subpolar gyre here is defined as the region between 45° and 65°N . Sensitivity studies made by changing the bounding latitudes by several degrees do not qualitatively change the results. Here we focus on P in winter months, since it dominates the annual power input (see Fig. 9a; Fig. 9 will be described in greater detail below). The first message from Fig. 3b is that power input to the subpolar North Atlantic varies significantly on

interannual time scales. The maximum P over this 140-yr period reaches $\sim 4.5 \times 10^{10}$ W in 1994, whereas P in 1969 is slightly negative ($\sim -9.6 \times 10^8$ W).

Coherence analysis shows that the time series of the winter NAO index and P are highly correlated at all frequencies at zero phase lag,² with a mean value of 0.73 (Fig. 4), suggesting that the winter NAO index is a good indicator for the amount of power input to the subpolar North Atlantic, accounting for roughly 50% of its variance; atmospheric winds inject more energy into the subpolar North Atlantic during positive NAO years. (Data used to compute the NAO index will have also been used in the reanalysis.)

Zhai et al. (2012) recently showed that the majority of the time-mean power input to the subpolar North Atlantic arises from synoptic winds. To understand their role in the variability of P seen in Fig. 3b, stresses associated with monthly winds, values of P_m (the thin line in Fig. 3b) are computed. Consistent with Zhai et al. (2012), the time-mean P_m makes a fractional contribution ($\sim 30\%$) to the time-mean P over the 140-yr period. In addition, the standard deviation of P_m over this period of time is $\sim 3.7 \times 10^9$ W, only about one-third of

² Both time series are detrended before coherence analysis.

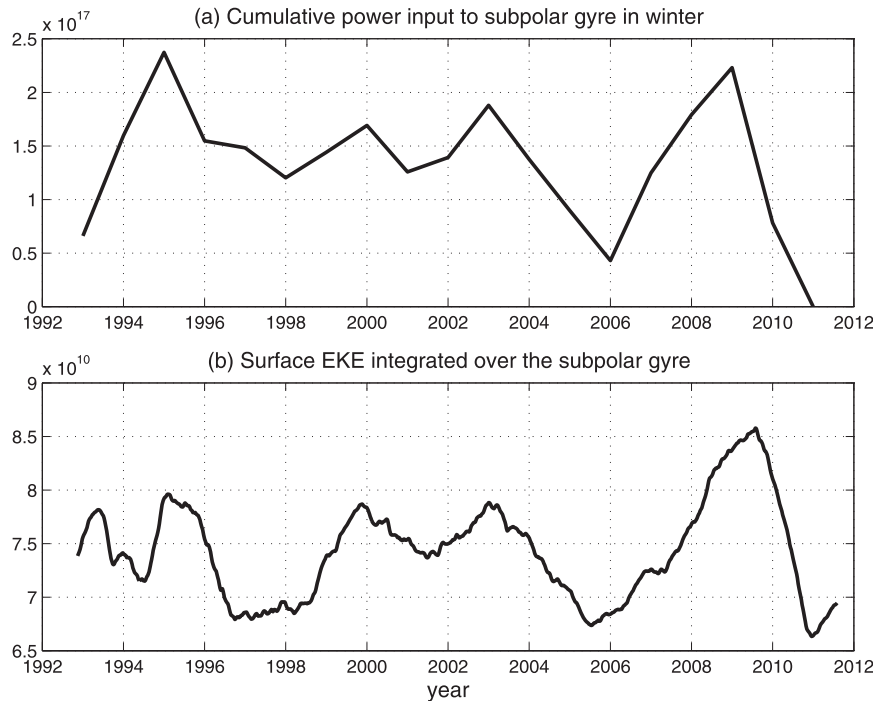


FIG. 8. (a) The cumulative power input to the subpolar North Atlantic in winter (J). Note that the time-mean value is removed before cumulation. (b) The EKE integrated over the subpolar North Atlantic and running averaged over a year ($\text{m}^4 \text{s}^{-2}$).

that associated with P ($\sim 9.1 \times 10^9 \text{ W}$). Thus, the variability of power input to the subpolar North Atlantic is mostly caused by variability of synoptic winds. In other words, the enhanced storm activities in the subpolar North Atlantic account for the greater power input there during positive NAO years. Readers are referred to Compo et al. (2011) [see also Donat et al. (2011) and Wang et al. (2013)] for estimates of storminess from 20CR. Useful estimates of paleoclimate ocean states presumably need to consider not just changes in large-scale winds, but also shifts in the properties of the storm tracks.

The ocean has an extended memory—tending to integrate the effects of external disturbances over long periods of time. As one indicator of the consequences of that integration, consider the cumulative power input to the subpolar North Atlantic Π , which shows pronounced multidecadal variability over the 140-yr period, with decreasing values during 1880–1900 and 1950–70 and increasing values during 1900–30 and 1980–2010 (Fig. 5a). Figure 5b shows the Atlantic multidecadal oscillation (AMO) index from Enfield et al. (2001), which is basically the area-weighted average of the Kaplan et al. (1998) sea surface temperature anomalies over the whole North Atlantic. The AMO index exhibits multidecadal variability similar to the power variations, with warm phases occurring

during 1860–80 and 1930–60 and cool phases during 1905–25 and 1970–90. Significant coherence exists between Π and the AMO index in frequency bands around 3 and 10 years and also at the very lowest frequencies, with corresponding phase shifts of about 180° , 90° , and 0° , respectively (Fig. 6).³ The zero phase relationship at the very lowest frequencies is what one sees visually. It is not clear what physical mechanisms are at work that link variability of Π and the AMO index in these distinct frequency bands. The frequency dependence of the phases strongly suggests that the physical processes acting are nonuniform with time scale. No causality between the processes is necessarily to be inferred from the evidence here, but a dependence of ocean circulation properties on the total power input over very long periods is consistent with the known long oceanic memory. No reason exists to believe that a calculation extending even as far back as 1871 is sufficiently long to describe the interval over which power accumulation or its deficit would influence what is observed.

³ The information content of the coherence between the AMO and P and that between the AMO and Π is identical—differing only in the calculated phases.

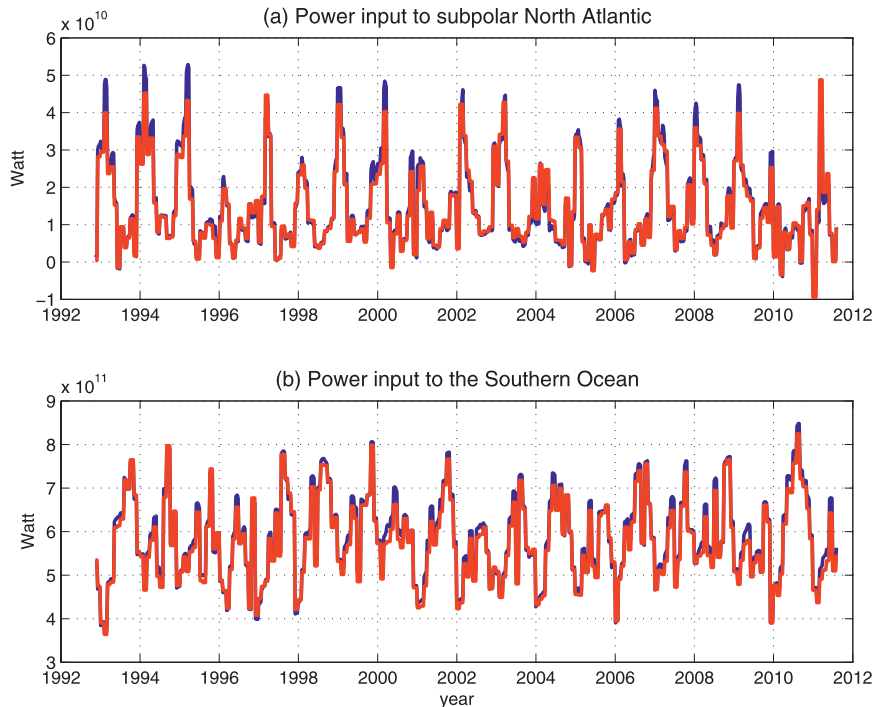


FIG. 9. (a) The red line is the power input to the subpolar North Atlantic estimated with the steady ocean circulation approximation P and the blue line is the power input estimated without the steady ocean circulation approximation \tilde{P} . (b) As in (a), but for the Southern Ocean.

c. Power input 1992–2011

For the period of 1992–2011, power input can be computed using time-varying surface ocean currents, relaxing the steady ocean circulation approximation.⁴ The accuracy of estimates of the variability of P calculated by ignoring changes in the oceanic surface flow can be accessed, at least for these two decades.

Including the time-varying ocean circulation power input \tilde{P} to the subpolar North Atlantic again varies significantly on interannual time scales for the period of 1992–2011 (Fig. 7b), and is significantly correlated with the winter NAO index (Fig. 7a). Note that \tilde{P}_m covaries with \tilde{P} , and the standard deviation of \tilde{P}_m over this period of time is again only about one-third of that associated with \tilde{P} , similar to that diagnosed for the period 1871–2010 using the 20CR product. This result further confirms the importance of winter storms in supplying energy to the subpolar North Atlantic and in causing its variability. It is worth noting that part of the stresses

owing to monthly winds may be an indirect result of the action of synoptic winds, because synoptic storms are known to strongly influence the low-frequency flow such as the monthly-mean fields at midlatitudes (e.g., Limpasuvan and Hartmann 1999; Jin et al. 2006).

The consequences of this significant interannual variability of power input are not understood. Some power going into the ocean results in the generation of eddies through instability processes (e.g., Gill et al. 1974; Wunsch 1998; Zhai and Marshall 2013). Here, the link to direct eddy generation is examined by computing the estimated coherence between P and eddy kinetic energy (EKE) in the subpolar gyre. Nonlocal effects such as advection of EKE across 45° and 65°N are excluded. EKE is defined here as $(\overline{u'^2 + v'^2})/2$, where u' and v' are geostrophic velocity anomalies derived from the SSH anomalies and the over bar denotes the running average over a year. Given the long integration times in the ocean, it is plausible that the accumulating power input Π controls the EKE variations on interannual time scales (Fig. 8).

Coherence between Π and EKE is almost uniform with a value of about 0.6, suggesting that about 35% of the variance is common to them and at zero phase lag (not shown). Determining the causes of the observed

⁴ Power input estimated using time-varying surface ocean circulation is labeled \tilde{P} here in order to distinguish it from that estimated with the steady ocean circulation approximation in the previous sections.

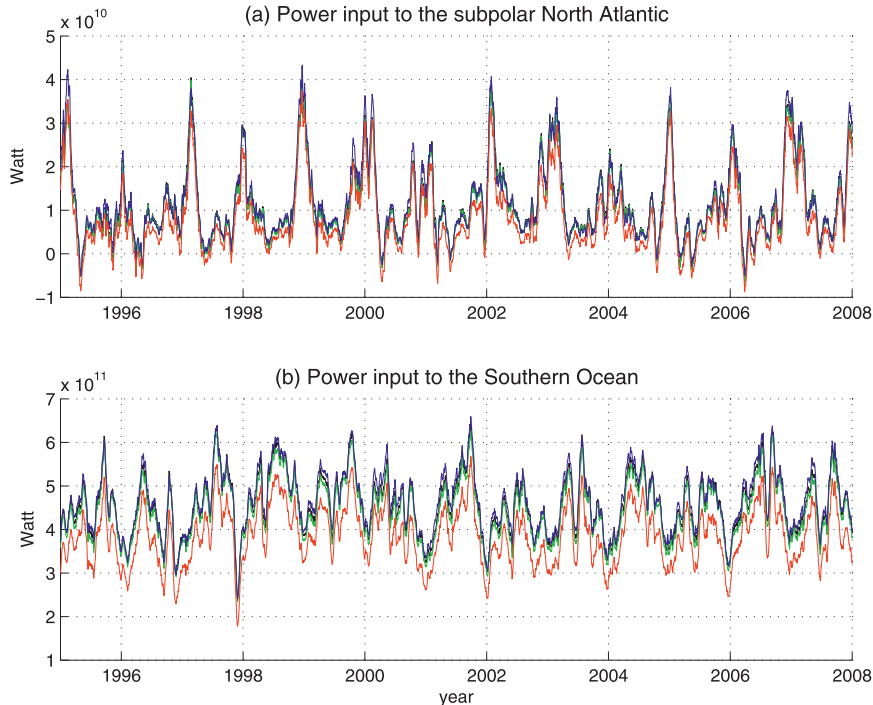


FIG. 10. Power input to (a) the subpolar North Atlantic and (b) the Southern Ocean calculated using the 6-hourly NCEP wind and four different methods. For details about the figure, including the meaning of the colored lines, please consult section 3c(2).

interannual eddy energy variability in the ocean is not straightforward. Stammer and Wunsch (1999) hypothesized that part of the EKE variability at high latitudes is caused by changes in local wind forcing. This hypothesis was examined by Penduff et al. (2004) using a $1/6^\circ$ model of the Atlantic Ocean, where they found the gyre-scale EKE fluctuations followed changes in wind energy input with a lag of about one year, suggesting that complex adjustment processes such as spinup/spindown of the gyre circulation may be involved [see also discussions in Stammer et al. (2006)]. The significant correlation between Π and EKE found in the present study is consistent with this picture, since it is the cumulative power input, not the instantaneous value, that spins the gyre circulation up or down.

1) STEADY OCEAN CIRCULATION APPROXIMATION

The accuracy of estimates of the variability of wind power input calculated by ignoring changes in the oceanic surface flow can be tested by comparing power input estimated with the steady ocean circulation approximation (i.e., P) with that estimated without (i.e., \tilde{P}) (Fig. 9). In the subpolar North Atlantic, P visually resembles \tilde{P} reasonably well, and the mismatch between them, measured by

$$\gamma = \frac{|P - \tilde{P}|}{\tilde{P}}, \quad (3)$$

is about 6% on average in winter. The mismatch in the Southern Ocean, where the wind injects most of its energy, is even smaller (<2%). Thus, the approximation is adequate at present levels of accuracy—where the errors are likely dominated by those in the wind stress estimates. As one would expect, P tends to slightly underestimate the variability of \tilde{P} (see also Lauderdale et al. 2012).

2) RESTING OCEAN APPROXIMATION

The resting ocean approximation—neglecting the ocean flow in the stress law—can be tested using the 6-hourly NCEP wind field. Following Zhai et al. (2012), surface wind stress is computed, both with the moving ocean effect and without, from 10-m wind using the Large et al. (1994) formula for the drag coefficient.

Figure 10 shows the power inputs calculated for the subpolar North Atlantic and the Southern Ocean using four different methods: 1) The blue line denotes power input without the moving ocean effect (i.e., $\tau_{\text{atmos-only}} \cdot \mathbf{u}_g$). 2) The black line is the same as the blue line, except the time-mean surface geostrophic velocity

is used (i.e., $\tau_{\text{atmos-only}} \cdot \mathbf{u}_{\text{gm}}$). 3) The red line denotes power input with the moving ocean effect (i.e., $\tau_{u_g} \cdot \mathbf{u}_g$). 4) The green line denotes power input with the moving ocean effect associated only with the time-mean surface currents (i.e., $\tau_{u_{\text{gm}}} \cdot \mathbf{u}_{\text{gm}}$).

There are a few noticeable features in Fig. 10. 1) Power inputs calculated using the 6-hourly wind systematically underestimate power input calculated using the monthly-mean wind stress (Fig. 9) because the monthly-mean wind stress includes contributions from wind variability at periods shorter than 6 h (Zhai et al. 2012). 2) The black line almost exactly overlaps with the blue line, confirming that treating the ocean circulation as steady is a good approximation when the moving ocean effect in the stress calculation is not considered. 3) The red line, although systematically lower than the blue line as expected, captures the majority of the variability of the blue line, suggesting that the variability of wind power input is indeed dominated by the changing wind, not the changing ocean circulation, at least on the accessible time scales. 4) The green line largely overlaps with the black and blue lines, demonstrating that the moving ocean effect is owing mostly to the ocean eddies.

4. Concluding remarks

The time-varying power input to the ocean by the wind field has been estimated using a reanalysis product over the interval 1871–2010.

- The 1871–2010 reanalysis of Compo et al. (2011) produces a calculated global power input to the ocean that increased by over 30% over the last 140 years. Most of the increase occurs in the Southern Ocean monthly wind stress and is inferred here to be almost surely an artifact of the changing observational base. This inference is consistent with the critiques of the reanalyses cited above—that the uncertainty of the changing climate state in these products lies primarily with the impact of major shifts in the database size and quality through time.

Restricting the analysis therefore, to the North Atlantic, leads to the following conclusions:

- Treating the ocean circulation as steady is a good approximation (accurate to a few percent).
- Power input to the subpolar North Atlantic varies significantly in time, covarying with the winter NAO index, being greater during positive NAO years owing to enhanced synoptic activity over the subpolar ocean.
- Eddy kinetic energy in the subpolar North Atlantic is significantly correlated with the cumulative power input there for the period from 1992 to 2011.

- Cumulative wind power input to the subpolar North Atlantic is significantly coherent with the AMO index in three distinct frequency bands with differing phases over the period from 1871 to 2010. The extent to which the data used to compute the AMO index are used in the reanalysis to calculate the wind field in the reanalysis is not known.

A final comment is that the importance of synoptic wind systems to stress calculations would be a particular problem in paleoceanographic studies—requiring knowledge not only of the large-scale wind patterns and strength, but also the storm tracks and disturbance intensities.

Acknowledgments. We wish to thank Patrick Heimbach for helpful discussions. CW thanks the American Rhodes Trust and Oxford University for support as George Eastman Visiting Professor, Balliol College and the Department of Physics, Oxford University. We thank David Straub, Anand Gnanadesikan, and two anonymous reviewers for valuable comments.

REFERENCES

- Bengtsson, L., S. Hagemann, and K. I. Hodges, 2004: Can climate trends be calculated from reanalysis data? *J. Geophys. Res.*, **109**, D11111, doi:10.1029/2004JD004536.
- Bromwich, D. H., and R. L. Fogt, 2004: Strong trends in the skill of the ERA-40 and NCEP–NCAR reanalyses in the high and midlatitudes of the Southern Hemisphere, 1958–2001. *J. Climate*, **17**, 4603–4619.
- , —, K. I. Hodges, and J. E. Walsh, 2007: A tropospheric assessment of the ERA-40, NCEP, and JRA-25 global reanalyses in the polar regions. *J. Geophys. Res.*, **112**, D10111, doi:10.1029/2006JD007859.
- , J. P. Nicolas, and A. J. Monaghan, 2011: An assessment of precipitation changes over Antarctica and the Southern Ocean since 1989 in contemporary global reanalyses. *J. Climate*, **24**, 4189–4209.
- Brown, J. N., and A. V. Fedorov, 2010: How much energy is transferred from the winds to the thermocline on ENSO time scales? *J. Climate*, **23**, 1563–1580.
- Compo, G. P., and Coauthors, 2011: The Twentieth Century Reanalysis Project. *Quart. J. Roy. Meteor. Soc.*, **137**, 1–28, doi:10.1002/qj.776.
- Donat, M. G., D. Renggli, S. Wild, L. V. Alexander, G. C. Leckebusch, and U. Ulbrich, 2011: Reanalysis suggests long-term upward trends in European storminess since 1871. *Geophys. Res. Lett.*, **38**, L14703, doi:10.1029/2011GL047995.
- Duhaut, T. H., and D. N. Straub, 2006: Wind stress dependence on ocean surface velocity: Implications for mechanical energy input to ocean circulation. *J. Phys. Oceanogr.*, **36**, 202–211.
- Enfield, D. B., A. M. Mestas-Nuñez, and P. J. Trimble, 2001: The Atlantic multidecadal oscillation and its relationship to rainfall and river flows in the continental U.S. *Geophys. Res. Lett.*, **28**, 2077–2080.

- Faller, A. J., 1966: Sources of energy for the ocean circulation and a theory of the mixed layer. *Proc. Fifth U.S. Congress of Applied Mechanics*, Minneapolis, MN, ASME, 651–672.
- Gill, A. E., J. S. A. Green, and A. J. Simmons, 1974: Energy partition in the large-scale ocean circulation and the production of mid-ocean eddies. *Deep-Sea Res.*, **21**, 499–528.
- Hazewinkel, J., F. Paparella, and W. R. Young, 2012: Stressed horizontal convection. *J. Fluid Mech.*, **692**, 317–331.
- Huang, R. X., W. Wang, and L. Liu, 2006: Decadal variability of wind-energy input to the World Ocean. *Deep-Sea Res.*, **53**, 31–41.
- Hughes, C., and C. Wilson, 2008: Wind work on the geostrophic ocean circulation: An observational study on the effect of small scales in the wind stress. *J. Geophys. Res.*, **113**, C02016, doi:10.1029/2007JC004371.
- Hurrell, J. W., 1995: Decadal trends in the North Atlantic Oscillation and relationships to regional temperatures and precipitation. *Science*, **269**, 676–679.
- Jin, F.-F., L.-L. Pan, and M. Watanabe, 2006: Dynamics of synoptic eddy and low-frequency flow interaction. Part I: A linear closure. *J. Atmos. Sci.*, **63**, 1677–1694.
- Kalnay, E., and Coauthors, 1996: The NCEP/NCAR 40-Year Reanalysis Project. *Bull. Amer. Meteor. Soc.*, **77**, 437–471.
- Kaplan, A., M. A. Cane, Y. Kushnir, A. C. Clement, M. B. Blumenthal, and B. Rajagopalan, 1998: Analyses of global sea surface temperatures 1856–1991. *J. Geophys. Res.*, **103**, 18 567–18 589.
- Large, W. G., J. C. McWilliams, and S. C. Doney, 1994: Oceanic vertical mixing: A review and a model with a nonlocal boundary layer parameterization. *Rev. Geophys.*, **32**, 363–403.
- Lauderdale, J. M., A. C. Naveira Garabato, K. I. C. Oliver, and L. N. Thomas, 2012: Climatic variations of the work done by the wind on the ocean's general circulation. *J. Geophys. Res.*, **117**, C09017, doi:10.1029/2012JC008135.
- Le Traon, P. Y., F. Nadal, and N. Ducet, 1998: An improved mapping method of multisatellite altimeter data. *J. Atmos. Oceanic Technol.*, **15**, 522–534.
- Limpasuvan, V., and D. L. Hartmann, 1999: Eddies and the annular modes of climate variability. *Geophys. Res. Lett.*, **26**, 3133–3136.
- Maximenko, N. A., and P. P. Niiler, 2005: Hybrid decade-mean global sea level with mesoscale resolution. *Recent Advances in Marine Science and Technology*, N. Saxena, Ed., PACON International, 55–59.
- Nicolas, J. P., and D. H. Bromwich, 2011: Precipitation changes in high southern latitudes from global reanalysis: A cautionary tale. *Surv. Geophys.*, **32**, 475–494.
- Penduff, T., B. Barnier, W. K. Dewar, and J. J. O'Brien, 2004: Dynamical response of the oceanic eddy field to the North Atlantic Oscillation: A model–data comparison. *J. Phys. Oceanogr.*, **34**, 2615–2629.
- Rayner, N. A., D. E. Parker, E. B. Horton, C. K. Folland, L. V. Alexander, D. P. Rowell, E. C. Kent, and A. Kaplan, 2003: Global analyses of sea surface temperature, sea ice, and night marine air temperature since the late nineteenth century. *J. Geophys. Res.*, **108**, 4407, doi:10.1029/2002JD002670.
- Roquet, F., C. Wunsch, and G. Madec, 2011: On the patterns of wind-power input to the ocean circulation. *J. Phys. Oceanogr.*, **41**, 2328–2342.
- Scott, R. B., and Y. Xu, 2009: An update on the wind power input to the surface geostrophic flow of the World Ocean. *Deep-Sea Res.*, **56**, 295–304.
- Stammer, D., and C. Wunsch, 1999: Temporal changes in eddy energy of the oceans. *Deep-Sea Res. II*, **46**, 77–108.
- , —, and K. Ueyoshi, 2006: Temporal changes in ocean eddy transports. *J. Phys. Oceanogr.*, **36**, 543–550.
- Stern, M. E., 1975: *Ocean Circulation Physics*. International Geographic Series, Vol. 19, Academic Press, 246 pp.
- Trenberth, K. E., J. W. Hurrell, and A. Solomon, 1995: Conservation of mass in three dimensions in global analysis. *J. Climate*, **8**, 692–708.
- , D. P. Stepaniak, J. W. Hurrell, and M. Fiorino, 2001: Quality of reanalyses in the tropics. *J. Climate*, **14**, 1499–1510.
- Wang, W., A. Köhl, and D. Stammer, 2010: Estimates of global ocean volume transports during 1960 through 2001. *Geophys. Res. Lett.*, **37**, L15601, doi:10.1029/2010GL043949.
- Wang, X. L., Y. Feng, G. P. Compo, V. R. Swail, F. W. Zwiers, R. J. Allan, and P. D. Sardeshmukh, 2013: Trends and low-frequency variability of extra-tropical cyclone activity in the ensemble of twentieth century reanalysis. *Climate Dyn.*, doi:10.1007/s00382-012-1450-9, in press.
- Wunsch, C., 1998: The work done by the wind on the oceanic general circulation. *J. Phys. Oceanogr.*, **28**, 2332–2340.
- , 2005: Thermohaline loops, Stommel box models, and the Sandström theorem. *Tellus*, **57A**, 84–99.
- , and R. Ferrari, 2004: Vertical mixing, energy, and the general circulation of the oceans. *Annu. Rev. Fluid Mech.*, **36**, 281–314.
- , and P. Heimbach, 2013: Dynamically and kinematically consistent global ocean circulation state estimates with land and sea ice. *Ocean Circulation and Climate*, 2nd ed. G. Sielder et al., Eds., Elsevier, in press.
- Zhai, X., and D. P. Marshall, 2013: Vertical eddy energy fluxes in the North Atlantic subtropical and subpolar gyres. *J. Phys. Oceanogr.*, **43**, 95–103.
- , H. L. Johnson, D. P. Marshall, and C. Wunsch, 2012: On the wind power input to the ocean general circulation. *J. Phys. Oceanogr.*, **42**, 1357–1365.